Polyglycolide: degradation and drug release. Part I: Changes in morphology during degradation

SUSAN HURRELL, RUTH E. CAMERON*
Department of Materials Science and Metallurgy, University of Cambridge, Pembroke Street, Cambridge, CB2 3QZ
E-mail: rec11@cam.ac.uk

The changing morphology of quenched polyglycolide (PGA) is investigated during hydrolytic degradation in phosphate buffered saline at pH 7.4. Analysis techniques include small and wide-angle X-ray scattering (SAXS and WAXS), mass measurements, DSC, pH measurement and UV-spectrophotometry. It is postulated that the degradation process can be separated into four distinct stages. In stage I, water diffuses quickly into the sample. During stage II, the polymer crystallizes by insertion crystallization, whilst the molecular weight gradually falls. This stage is characterized by a dramatic fall in the long period together with an increase in the crystallinity, minimal mass loss and minimal water uptake. At the onset of stage III, at around 10 days, a critical molecular weight is reached. Degradation products are now small enough to diffuse from the surface of the sample which begins to swell, water diffuses into the space created, and the crystals are freed from constraint. A co-operation between degradation products diffusing out of the sample and the water diffusing in causes ''reaction–erosion'' fronts to develop inside the sample. Ahead of these fronts, the trapped acidic degradation products remain to catalyze the hydrolysis. Stage III is characterized by swelling and an increase in the long period, together with mass loss and further water uptake. It is postulated that these reaction–erosion fronts move through the sample and meet in the centre at the beginning of stage IV, at which point the degradation again becomes homogeneous throughout the sample.

1. Introduction

Previous work on the hydrolysis of simple unoriented poly(α-hydroxyacids) for drug delivery has focused on polylactide-based copolymers and stereocopolymers. PGA has generally been disregarded as a potential matrix for the controlled delivery of drugs due to its insolubility in all common organic solvents and high melting point, and no detailed model of the effects of hydration and degradation on morphology has been proposed. However it is biocompatible, is used for degradable sutures, and has a hydrolysis rate suitable for many drug release applications.

The extensive literature on the hydrolysis and drug release rates of (mostly lactide containing) poly(α-hydroxyacids) reveals the complexity of the hydrolysis mechanism, which depends on many variables such as crystallinity [1–13], sample size and shape [6, 10, 14–16] and the nature of the degradation medium [2, 4, 17–26]. In this paper, quenched PGA samples are analyzed at various stages of degradation to elucidate the effects of hydrolysis on the morphology.

2. Materials and methods

Small pellets of PGA with an intrinsic viscosity of 1.2 dl/g were obtained from Medisorb Technologies International, Ohio. Samples of mass 36 ± 1 mg were ground and then melted in DSC pans on a Linkam hotstage at 236 °C. The samples were quenched in iced water, and removed from the pans. Phosphate buffered saline of pH 7.4 and concentration 0.01 M was prepared using tablets from Sigma-Aldrich. The samples were placed in bottles containing 20 ml of buffer solution at regular time intervals and the bottles were placed into a water bath without agitation at 37 °C. All samples were analyzed wet.

The average diameters of the samples were measured on graph paper by taking photographs before and after degradation using a WILD Heerbrugg stereo microscope.

X-ray analysis of wet degraded samples was performed on station 8.2 at the Daresbury SRS. SAXS and WAXS data were recorded simultaneously in 30-s frames. The WAXS data were collected on a curved INEL detector and the SAXS data on a quadrant detector.

*Corresponding author.

All data were normalized to even out the effects of fluctuations in the beam intensity and the thickness of the samples, and divided by the response of the detector to an even ^{55}Fe irradiation. Background scattering was subtracted. Calibration of scattering angles was carried out using high-density polyethylene and wet rat-tail collagen for the WAXS and SAXS data respectively. The Lorentz correction was applied to the SAXS data to convert the scattering from lamellar stacks at all possible orientations to that predicted from a single lamellar stack. The long period, or average lamellar repeat distance (d) of the semicrystalline polymer was then calculated from the peak positions (at scattering vector q) using the following equation:

$$d = \frac{2\pi}{q} \tag{1}$$

Crystallinity was calculated from the corrected WAXS profiles by measuring the area under the crystal peaks and dividing by the total area under the curve.

To find the mass loss and water content of PGA samples as a function of degradation time, the samples were weighed three times: initially; wet after degradation; and again after drying. The initial mass was measured to an accuracy of $\pm$ 0.001 mg. The samples were then degraded, dabbed dry with a tissue and weighed immediately with an accuracy of $\pm$ 0.01 mg. The samples were then placed in a vacuum oven at 50 °C for 3 days and weighed again giving the dry mass accurate to $\pm$ 0.001 mg. The mass loss is calculated by subtracting the original mass from the dried mass, and the water content is calculated by subtracting the dried mass from the wet mass. Both results are expressed as a percentage of the original mass.

The glass transition temperatures (T_g) of wet samples, which had been degraded for up to 2 days, were measured using a Perkin Elmer DSC calibrated with an indium standard. Samples were dried with a tissue, placed in aluminum pans and heated from -10 °C to 70 °C at 10 °C/min.

The concentration of glycolic acid was calculated using a technique described by Chu and Louie [27]. Chromotropic acid disodium salt, necessary for this analysis, was obtained from Fisher Scientific; glycolic and sulfuric acids were obtained from Sigma-Aldrich. A Uvikon 860 double beam spectrophotometer was used for the UV analysis. An electronic hand-held pH meter was used to measure the pH to an accuracy of $\pm$ 0.5.

3. Results

The quenched amorphous samples were almost transparent and very hard. As degradation proceeded they became more cloudy and brittle, and began to disintegrate. The thickness of the samples varied across individual samples and between different ones, and was approximately 0.5 mm for the first 10 days, increasing to approximately 0.6 and 0.8 mm after 20 and 27 days respectively. The diameters of the wet samples remained constant for 10 days and then gradually increased (Fig. 1). These samples were dried in a vacuum oven at 50 °C for 3 days and photographed again. Fig. 2 shows that the

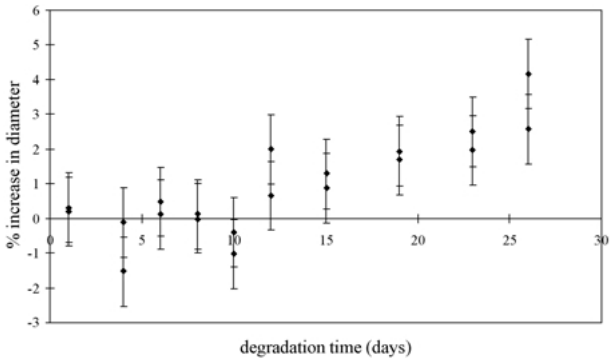

Figure 1 The percentage change in the diameter of samples measured wet after degradation. Initial diameters are between 6 and 7 mm. The errors are estimated at approximately $\pm$ 1%.

dry sample diameters began to decrease dramatically between 15 and 20 days. When the scales of Figs 1 and 2 are compared, it is clear that after 15 days the water serves to maintain the skeleton structure of the sample. When the water is removed, the sample shrinks dramatically.

One of the most important problems associated with PGA is its insolubility in all common organic solvents. It has therefore proved impossible to measure changes in molecular weight, even though this has been perhaps one of the most important techniques employed for characterizing other degradable polymers.

Three observations can be made from the SAXS data presented in Figs 3 and 4. The first is that the peak position moves to higher angles during the first 10 days and then moves back again. Long period results (Fig. 5) therefore show a dramatic fall over the first 10 days and a subsequent increase. The second is that the intensity of the peak increases during degradation. The third is that after 10 days the intensity at very low angles begins to increase more dramatically, and to dominate the peak.

Fig. 6 is a typical example of the effect of degradation on the WAXS profile. The peaks are indexed according to an orthorhombic unit cell. As degradation proceeds, the intensities of the crystal peaks increase with respect to the amorphous halo. The amorphous halo, which has a maximum at around 20° 2-theta, decreases in intensity and another crystal peak becomes visible on top of it. A second ''amorphous halo'' at around 29° 2-theta becomes increasingly intense, and is probably a result of nearest-neighbour scattering from atoms within the

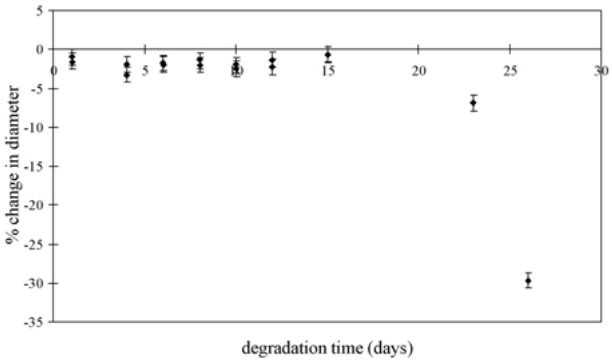

Figure 2 The percentage change in the diameters of samples measured wet and then dried in a vacuum oven for 3 days.

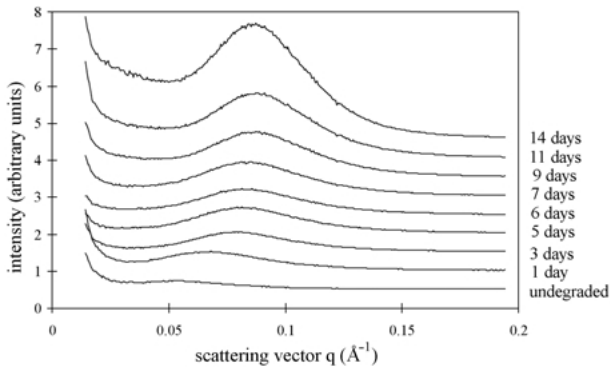

Figure 3 SAXS Profiles of degrading PGA. The curves are offset for clarity.

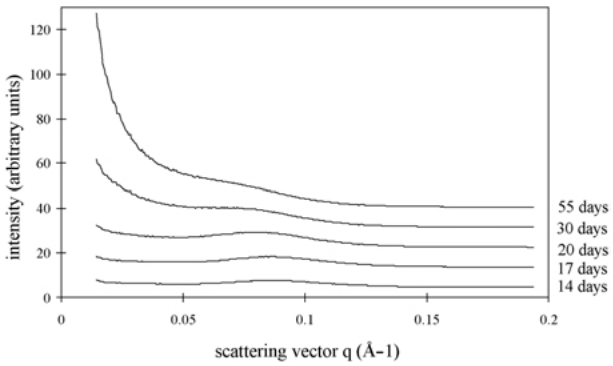

Figure 4 SAXS profiles of degrading PGA. The curves are offset for clarity.

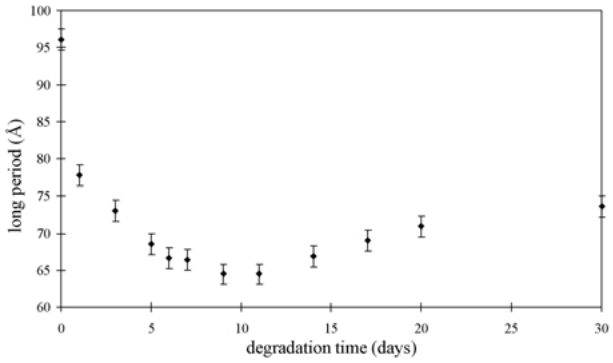

Figure 5 Long Period changes with increasing degradation.

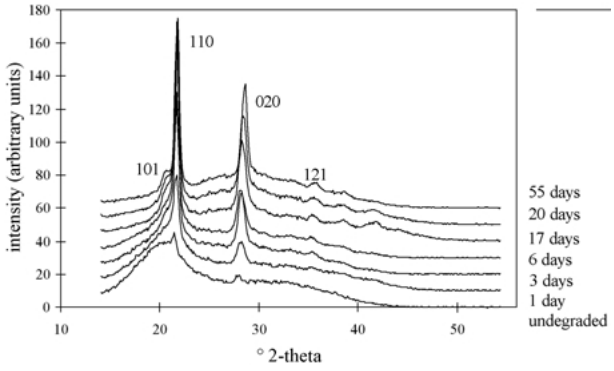

Figure 6 WAXS profiles of degrading PGA.

polymer chains and water molecules. According to Bernal and Fowler [28], WAXS profiles from pure water show a first maximum at 27.3° 2-theta. Fig. 7 shows the crystallinity increasing over the first 10 days, reaching around 30% and then leveling off, but this low value is probably affected by water which is present in the amorphous regions of the polymer; the scattering from water is being measured along with the amorphous halo.

The (1 1 0) and (0 2 0) peak positions are plotted against degradation time in Figs 8 and 9. The peak positions only change slightly, which implies that the crystals remain relatively undisturbed and that the degradation is occurring predominantly in the amorphous phase or at the crystal surfaces. This is to be expected since water is a large molecule compared with the interstices of the crystal. However, there is a slight increase after 10 days of degradation: the (1 1 0) peak moves from 21.6 to 21.8° 2-theta, an increase of 0.2° 2-theta (lying within the error bars); the (0 2 0) peak moves from 28.2 to 28.6° 2-theta, an increase of 0.4° 2-theta. This small increase in peak positions arises from a small decrease in the unit cell parameters; particularly in b: the unit cell parameters a and b decrease by 0.06 (1.1%) and 0.08 (1.3%) respectively. This indicates an increasing crystal perfection, which may arise from the removal of tie-chains during degradation.

The effect of a few hours of degradation on the glass transition temperature (T_g) of PGA is shown in Fig. 10. Degradation times of longer than two days were not investigated, since the samples had begun to crystallize

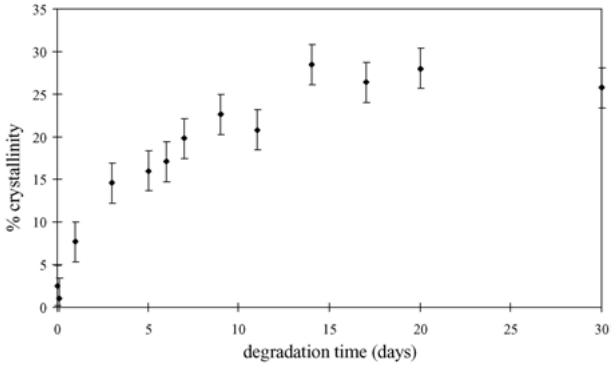

Figure 7 Changes in crystallinity with degradation.

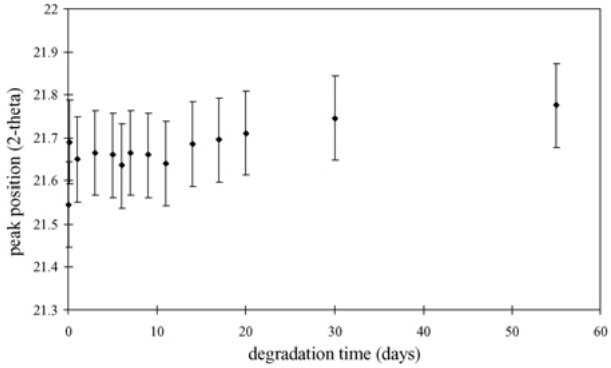

Figure 8 Changes in the position of the (1 1 0) WAXS peak with degradation. Error bars are included to specify the resolution (in pixels) of the original data.

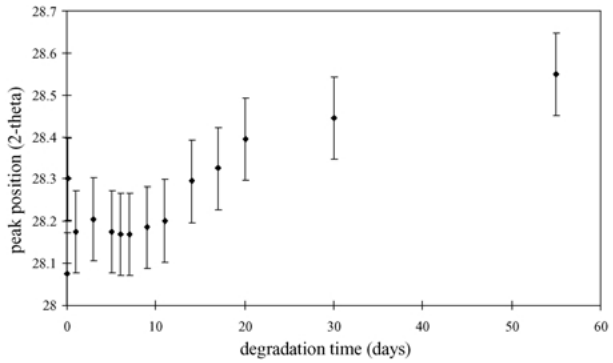

Figure 9 Changes in the position of the (0 2 0) WAXS peak with degradation. Error bars are included due to the resolution in pixels of the original data.

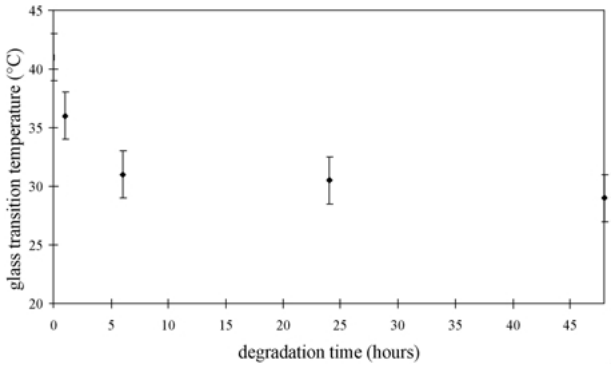

Figure 10 Changes in the glass transition temperature during the first two days of degradation. T_g was found to vary between approximately $\pm$ 2 °C.

and the T_g of these samples was therefore indistinct. The glass transition temperature falls quickly over the first 6 h and then continues to fall at a lower rate. This may indicate that water has diffused to the centre of the undegraded polymer structure in just 6 h, plasticizing the polymer and causing T_g to fall. This time scale compares well with a published diffusion constant of water in PGA of $(5 \pm 1) \times 10^{-9}$ cm^2 s^{-1} [20].

Fig. 11 shows the mass loss and water uptake profiles of the samples during degradation. During the first 10 days, the dry mass of the samples increases slightly, which must be due to an incomplete removal of tightly bound water in the structure. It is difficult to say how much water is being retained in the structure on drying and the results may therefore give an underestimate of the true mass loss. The water content increases slowly in the first 10 days. After 10 days both the mass loss and the

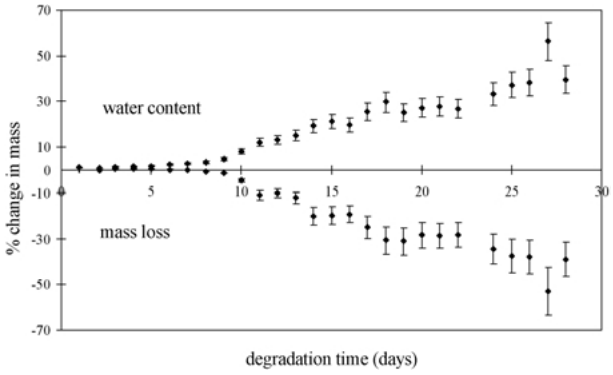

Figure 11 Changes in sample mass and water content with degradation.

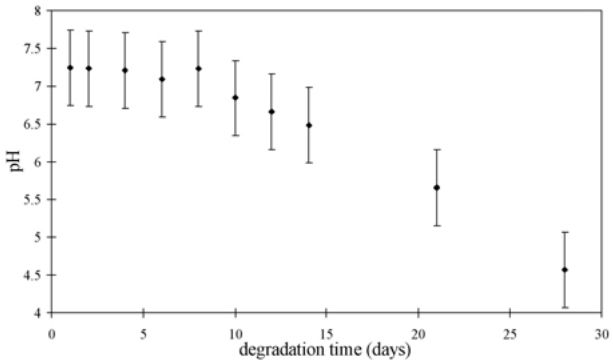

Figure 12 The pH of the buffer solutions changing with degradation.

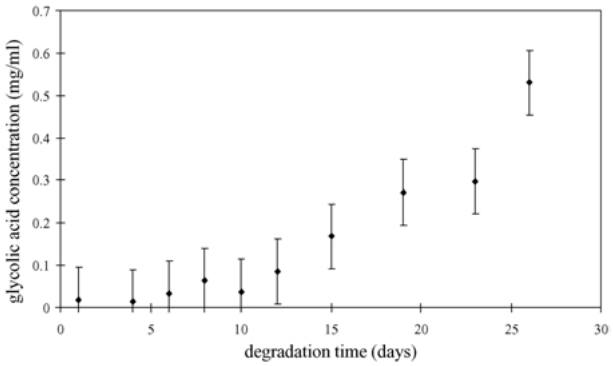

Figure 13 Glycolic acid content of solutions in which PGA samples had been degrading. The results were accurate to within an estimated $\pm$ 0.08 mg/ml.

water content increase more dramatically, until about 20 days when the rate decreases again. At this point, the results become rather unreliable since the samples are very brittle and material may be lost when the samples are dried. However, this should cause the mass loss to appear greater than it really is, and the results therefore certainly indicate that the rates of mass loss and water uptake are decreasing at this point.

The samples were degraded in only 20 ml of weakly buffered solutions. The pH of the solutions was tested at regular intervals with a pH meter to ensure that the buffer capacity was not reached. Fig. 12 shows a dramatic drop in pH after about 10 days. This must be due to the production of glycolic acid which is counteracting the buffer action.

The concentrations of glycolic acid in the buffer solutions are shown in Fig. 13. Some glycolic acid is present at the earliest stages, but its concentration increases more dramatically after 10 days. This indicates that some mass is lost from the samples during the first 10 days, even though this is not evident from the mass loss measurement.

4. Discussion

The results reveal a discontinuity in the behavior of degrading PGA at around 10 days, after which the size of the sample increases, the mass of the polymer falls, the water content rises, and the concentration of glycolic acid increases. At 10 days, a minimum in the long period is measured from the SAXS profiles. WAXS on the other hand shows an increase in crystallinity from the point at which the sample is immersed. These X-ray results will be considered first.

In an earlier paper [29], SAXS and WAXS results revealed a similar fall and rise in the long period and a similar increase in crystallinity to those observed in this study. Three physical mechanisms were identified which might explain the changes in the long period. These will now be considered in the light of the evidence presented in this paper.

The first mechanism postulated that the amorphous material is removed in two stages. Amorphous tie chains connect the lamellar crystals and it was proposed that the more taut tie chains are less reactive to hydrolysis than loosely coiled material. The loosely coiled polymer degrades and is removed from the sample, which causes the taut polymer chains to relax to more entropically favorable conformations, and the structure to contract. Eventually tie chains are also hydrolyzed and osmotic forces cause the sample to swell and the long period to increase again. This mechanism was originally developed to explain changes in the long period of pre-crystallized rather than quenched amorphous samples, but was extended to quenched samples. This model would explain the SAXS and WAXS results, but it is not easy to explain why taut polymer chains should be degraded more slowly than loosely-coiled material. However, the data presented here allows the model to be rejected. If such a dramatic fall in the long period is to be explained by the removal of amorphous material, it should also be accompanied by a significant loss of mass. The results in Fig. 11 show that this is not the case, and that very little mass is lost during the first 10 days when the long period is decreasing. Alternative mechanisms must therefore be considered.

The second mechanism suggested in King *et al*. [29] concerns crystallization of some of the amorphous material in the sample. A combination of nucleation and insertion secondary crystallization would produce the increase in crystallinity and dramatic fall in long period observed. For example, if one new crystal appears between two existing ones, the long period in that particular region is halved. This mechanism is consistent with the minimal mass loss of the polymer observed in this period. Rapid quenching will not allow a well-developed crystal structure to form. It is likely that plasticizing effects of water and the chain cleavage will allow new crystals to nucleate within existing lamellae, particularly during the early stages of degradation. ''Insertion secondary crystallization'' describes growth onto the lateral surfaces of existing crystals and since it is a more energetically favorable process, it is possible that it dominates later.

Insertion crystallization, however, cannot explain the later rise in long period, nor the associated increases in diameter, water content, mass loss, glycolic acid content and pH of the buffer solution. To do this, the ideas behind the third physical mechanism discussed in [29] must be developed. This mechanism proposes that parts of the structure might develop an increased affinity for water as a consequence of degradation, giving rise to swelling.

The papers of Vert *et al*. [1, 2, 6, 30] introduce the idea of heterogeneous bulk erosion to describe the degradation of poly(lactide)-based homopolymers and copolymers. This is based on a discontinuity in mass loss, water uptake and pH measurements after about 5 weeks for P(D,L)LA, and also the formation of a whitish layer on the surface of the samples after around 3 weeks. In addition, they find that the molecular weight is higher in this surface layer than in the centre of the sample. They postulate that homogeneous degradation occurs during the first stage. After some time a critical molecular weight is reached after which the degradation becomes heterogeneous. Long oligomers are formed with acidic end-groups, which are unable to diffuse from the centre of the sample and remain to catalyze the hydrolysis. At the surface however, the oligomers can pass into solution, leaving a porous region with a lower concentration of acidic end-groups and a higher average molecular weight. In the absence of acid catalysis this surface region will be hydrolyzed more slowly. Fig. 14 summarizes this idea.

PGA samples do not show a distinct surface layer forming during degradation. However, even if such a layer were formed, it may not be readily visible for two reasons: the samples become opaque over the first few days as the crystal structure develops; and PGA does not swell dramatically in any case, because it is constrained by the developing crystal structure. However, all other results in this paper indicate that PGA degrades in a very similar way to PLA-based homopolymers and copolymers, and we therefore postulate that a similar porous surface layer develops on the surface of PGA samples.

The higher concentration of free water in the surface layer would increase the mobility of all species, and as degradation products are removed, water molecules would be absorbed and take their place. This co-operative effect is likely to produce the sharp front between the dense polymer in the centre and the porous polymer on the surface, which is visible in the copolymers. These fronts, forming on each side of the sample, may be termed reaction–erosion fronts. The swollen porous material behind the fronts increases the average long period, increases the diameter of the sample and facilitates the absorption of water. Oligomers diffuse from the surface of the sample increasing the mass loss, and decreasing the pH as they are hydrolyzed further to glycolic acid in solution.

As degradation proceeds, the mass loss and water uptake continue, the long period continues to rise and the concentration of glycolic acid in the solution continues to increase. These results may be explained by a forward progression of the reaction–erosion fronts through the sample, which would increase the fraction of porous, water-swollen surface material. This would explain the continued rise in the long period. It would also give the

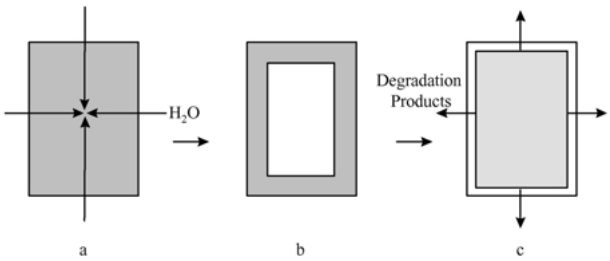

Figure 14 Schematic diagram of heterogeneous bulk erosion: (a) water diffuses into the sample; (b) degradation products build up in the center of the sample, autocatalyzing the reaction; (c) oligomers diffuse through the outer, less-degraded shell when their molecular weights are sufficiently low.

increasingly intense SAXS scatter at low angles characteristic of porous material. It is possible that the fronts meet in the centre of the sample at a later stage, which is consistent with the slower rate of water uptake and mass loss after 20–25 days.

The degradation profile can be summarized in four stages. Stage I occurs during the first 6 h, where buffer solution diffuses homogeneously into the sample. This is characterized by a fall in the glass transition temperature. Stage II describes the subsequent homogeneous hydrolysis of the polymer and continues until around 10 days. During this stage very little mass is lost, and water uptake is slow. After about 10 days a critical molecular weight is reached and stage III begins. As oligomers diffuse from the surface a reaction–erosion front forms, separating the central autocatalyzing region from the surface where oligomers begin to diffuse out. As oligomers diffuse out, space is created in the surface layer and more water diffuses in.

The progressive mass loss and swelling after the onset of stage III suggest that the fronts may move through the sample towards the centre, perhaps meeting at some time later, at a point termed stage IV. The evidence presented here is consistent with a movement of fronts towards the centre of the sample, but does not prove the idea. An exploration of the effects of sample geometry and size would give further insights into the validity of this hypothesis.

As well as confirming that heterogeneous bulk erosion occurs in PGA as well as PLA-based polymers, we have shown that SAXS is a good method for characterizing degrading semi-crystalline polymers. In subsequent papers, SAXS results will be used to probe the differences between the degradation profile of samples with different thermal histories, different sizes, and those degraded in different buffer solutions. The measured long period is an average over the whole sample and the minimum therefore arises from a balance between insertion crystallization and swelling behind the reaction–erosion fronts. At 10 days, the reaction–erosion front has begun to form and the swelling of the surface layer dominates insertion crystallization as the main mechanism affecting the overall long period. In the following paper we will show how the incorporation of a model drug into PGA affects the degradation behavior and how the drug release correlates with the degradation profile.

5. Conclusions

A four stage reaction-erosion front mechanism is proposed to describe the degradation of PGA matrices in buffer solution. Water diffuses quickly throughout the bulk of the sample in stage I. In stage II, homogeneous degradation occurs while the sample crystallizes through insertion crystallization facilitated by chain cleavage and water plasticization. At stage III a critical molecular weight is reached, oligomers begin to diffuse from the surface and a reaction–erosion front forms at the surface. We suggest that the front moves through the sample, perhaps meeting with the front from the opposite surface at stage IV.

Acknowledgments

The authors are grateful to Pfizer Ltd and the EPSRC for financial support, and to Dr Julie Richardson and Dr Hiep Huatan for help and advice. The X-ray experiments were carried out at the Daresbury Laboratory with the assistance of Dr B. U. Komanschek.

References

1. S. M. LI, H. GARREAU and M. VERT, *J. Mater. Sci. (Mater. in Med.)* **1** (1990) 123.
2. S. M. LI, H. GARREAU and M. VERT, *J. Mater. Sci. (Mater. In Med.)* **1** (1990) 131.
3. D. W GRIJMPA, A. J NIJENHUIS and A. J. PENNINGS, *Polymer* **31** (1990) 2201.
4. C. C. CHU, *J. Biomed. Mat. Res.* 1981 **15** (1981) 795.
5. D. K. GILDING and A. M. REED, *Polymer* **20** (1979) 1459.
6. S. M. LI, H. GARREAU and M. VERT, *J. Mater. Sci. (Mater. in Med.)* **1** (1990) 198.
7. R. J. FREDERICKS, A. J. MELVEGER and L. J. DOLEGIEWITZ, *J. Polym. Sci.* **22** (1984) 57.
8. J. W. LEENSLAG, A. J. PENNINGS, R. R. M. BOS, F. R. ROSEMA and G. BOERING *Biomaterials* **8** (1987) 311.
9. C. C. CHU, *J. Appl. Polym. Sci.* **26** (1981) 1727.
10. R. M. GINDE and R. K. GUPTA, *J. Appl. Polym. Sci.* **33** (1987) 2411.
11. A. BROWNING and C. C. CHU, *J. Biomed. Mat. Res.* **20** (1986) 613.
12. A. BROWNING and C. C. CHU, *J. Biomed. Mat. Res.* **20** (1988) 699.
13. R. A. MILLER, J. M. BRADY and D. E. CUTRIGHT, *J. Biomed. Mat. Res.* **11** (1977) 711.
14. P. TORMALA, H. M. MIKKOLA, J. VASENIUS, S. VAINIONPAA and P. ROKKANEN, *Die Angewandte Makromolekulare Chemie* **185** (1991) 293.
15. G. E. VISSCHER, J. E. PEARSON, J. W. FONG, G. J. ARGENTIERI and R. L. ROBISON, *J. Biomed. Mat. Res.* **22** (1988) 733.
16. M. VERT, S. M. LI, G. SPLENLEHAUER and P. GUERIN, *J. Mat. Sci.: Mater. in Medicine* **3** (1992) 432.
17. D. F. WILLIAMS and E. MORT, *J. Biomed. Mat. Res.* **14** (1980) 329.
18. R. A. KENLEY, M. O. LEE, T. R. MAHONEY and L. M. SANDERS, *Macromolecules* **20** (1987) 2398.
19. K. MAKINO, H. OHSHIMA and T. KONDO, *J. Microencapsulation* **3** (1986) 203.
20. G. E. ZAIKOV *JMS-REV. Macromol. Chem. Phys.* **C25** (1985) 551.
21. C. C. CHU, *J. Biomed. Mat. Res.* **15** (1981) 19.
22. E. A. SCHMITT, D. R. FLANAGAN and R. J. LINHARDT, *Macromolecules* **27** (1994) 743.
23. L. PRATT, C. CHU, J. AUER, A. CHU, J. KIM, J. A. ZOLLWEG and C. C. CHU, *J. Polymer Science: Part A: Polymer Chemistry* **31** (1993) 1759.
24. A. BRUNNER, K. MADER and A. GOPFERICH, *Int'l. Symp. Control. Rel. Bioact. Mater.* 1998.
25. K. FU, D. W. PACK, A. LAVERDIERE, S. SON and R. LANGER *Int'l Symp. Control. Rel. Bioact. Mater.* 1998.
26. A. M. REED and D. K. GILDING, *Polymer* **22** (1981) 494.
27. C. C. CHU and M. LOUIE, *J. Appl. Polym. Sci.* **30** (1985) 3133.
28. J. D. BERNAL and R. H. FOWLER *Journal of Chemical Physics* **1** (1933) 515.
29. E. KING, S. ROBINSON and R. E. CAMERON, *Polymer International* **48** (1999) 15.
30. I. GRIZZI, H. GARREAU, S. LI and M. VERT, *Biomaterials* **16** (1995) 305.

Received 31 March
and accepted 26 December 2000